

**Figure 4.** Plot of polycarbonate block length ( $\bar{n}_x$ ) as a function of end-capping ratio for a polymer which is 50 wt % PDMS and has a PDMS block length  $\bar{n}_D = 9.3$ . (Courtesy of S. Y. Hobbs.)

in Table I. Two sets of experimental data which were obtained from the same spectrum but different plot widths for the quaternary aliphatic carbon region are presented for each sample in order to show the reproducibility of these measurements. The largest deviation from the calculated polycarbonate block length occurs for the materials prepared with  $a/m = 1.2$ . The most likely reason for this is the extreme sensitivity of  $\bar{n}_x$  to  $a/m$  in this region. As depicted graphically in Figure 4, slight errors in measuring  $a/m$  between 1.1 and 1.8 will generate large deviations from the expected  $\bar{n}_x$ . The deviation of  $\bar{n}_x$  ( $^{13}\text{C}$ ) from the expected value in sample C ( $\bar{n}_D = 9.3$  and  $a/m = 1.2$ ) can be accounted for by assuming an end-cap ratio of 1.47 instead of 1.2. Likewise, sample F would have an average block length of about 22 if the end-cap ratio had actually been 1.4. Variation in composition from 50 wt % silicone also affects  $\bar{n}_x$ . The value of  $\bar{n}_x$  obtained from the  $^{13}\text{C}$  NMR spectrum is much closer to the calculated value (for  $a/m = 4$  and 2, samples A, B, D, and E) when the calculation is corrected to account for the actual composition of the polymer as determined by silicon analysis.

The information available from  $^{13}\text{C}$  NMR spectroscopy affords a means of monitoring the actual composition of these copolymers, regardless of variations in synthesis or uncertainties in measured quantities. It therefore provides a more direct analysis of these systems for studies of the

effects of structural changes on properties. Samples C and D, for example, were designed to differ in average BPAC sequence length by five units (12.3 and 7.0, respectively). By  $^{13}\text{C}$  NMR, however, they were found to have the same BPAC block length ( $\sim 8.5$ ) and thus should have the same domain size according to the physical model of Niznik and LeGrand.<sup>3</sup> A significantly higher amount of the BPA in polymer C is tied up in PDMS-BPA oligomers, and as a result the volume fraction of these domains in C should be smaller than in D. Also, the average PDMS-BPA oligomer in C contains three silicone blocks ( $\bar{n}_D = 9.3$ ) and two BPA links. Sample D has very few isolated BPA units and therefore the silicone portion of the polymer is largely comprised of chains with the starting siloxane chain length,  $\bar{n}_D = 18.4$ . These results are consistent with a higher modulus and tensile strength which was observed for D.

## Experimental Section

**Polymers.** Samples A-F were obtained from Dr. G. E. Niznik and were prepared according to published procedures.<sup>3</sup>

**NMR Measurements.** The  $^{13}\text{C}$  NMR spectra were obtained on a Varian FT-80A NMR spectrometer operating at 20 MHz for  $^{13}\text{C}$ . All spectra were acquired with complete proton decoupling and with deuterated solvents for field/frequency control (lock). Samples were doped with ca. 0.1 M tris(acetylacetonato)chromium to shorten the  $T_1$ 's and suppress the NOE.<sup>4</sup> A gated decoupling sequence and 2-s pulse delay were used to eliminate any residual NOE and allow for complete relaxation of all carbon nuclei. Typical spectral parameters were 4000-Hz spectral width, pulse width corresponding to a  $45^\circ$  flip angle, 1-s acquisition time, and 2-s pulse delay. The 16K data points allowed for 8K output data points in the transformed spectrum. The BPA quaternary aliphatic carbon region of each spectrum was plotted at 57- and 33-Hz plot widths. Quantitative determinations were made by measuring peak areas with a Zeiss MOP-3 image analyzer to give the data shown in Table I. Chemical shifts are reported in ppm relative to  $\text{Me}_4\text{Si}$  with positive values downfield.

**Acknowledgment.** We thank Drs. D. G. LeGrand and S. Y. Hobbs for very helpful discussions.

## References and Notes

- (1) Vaughn, H. A., Jr. *J. Polym. Sci., Part B* 1969, 7, 569.
- (2) Williams, E. A.; Cargioli, J. D.; Hobbs, S. Y. *Macromolecules* 1977, 10, 782.
- (3) Niznik, G. E.; LeGrand, D. G. *J. Polym. Sci., Polym. Symp.* 1977, No. 60, 97.
- (4) Gansow, O. A.; Burke, A. R.; Vernon, W. D. *J. Am. Chem. Soc.* 1972, 94, 2550.

## Measurement of the Polymer-Bound Fraction at the Solid-Liquid Interface by Pulsed Nuclear Magnetic Resonance

K. G. Barnett, T. Cosgrove,\* B. Vincent, and D. S. Sissons

School of Chemistry, University of Bristol, Bristol BS8 1TS, United Kingdom

M. Cohen-Stuart

Agricultural University, Wageningen, The Netherlands. Received December 12, 1980

**ABSTRACT:** Pulsed nuclear magnetic resonance (NMR) techniques have been used to estimate the polymer-bound fraction,  $\langle p \rangle$ , at solid surfaces in both aqueous and nonaqueous dispersions. The measured values are consistent with estimates of the strength of the polymer/substrate interaction energy. Spectra have also been obtained for a terminally anchored polymer.

## Introduction

Several experimental techniques now exist for measuring the fraction of segments of an adsorbed polymer that lie in an interfacial plane (trains). These techniques include

infrared (IR),<sup>1</sup> microcalorimetry,<sup>2</sup> and electron spin resonance (ESR).<sup>3</sup> Although good agreement has been found between microcalorimetry and IR<sup>2</sup> measurements, the ESR method gives substantially higher values for the number

of bound segments than IR.

NMR techniques have been used to estimate the bound fractions of polymers in solid dispersions<sup>4,5</sup> but in this paper a new NMR analysis sequence is outlined, with specific reference to liquid dispersions, and the results are compared with recent ESR and IR measurements.

Physically adsorbed polymers have been studied in both aqueous and nonaqueous dispersions and a terminally anchored polymer has been studied in a nonaqueous dispersion.

### Theoretical Background

Both the ESR and NMR methods for measuring the fraction,  $\langle p \rangle$ , of segments of an adsorbed polymer in trains rely on the premise that the polymer segments in trains have a greatly reduced mobility compared to free segments. This means that the correlation time for segments in trains,  $\tau_{tr}$ , is much greater than for loops and tails ( $\tau_{lt}$ ).  $\tau_{lt}$  should be of the same order as a polymer segment in concentrated solution. The ability to resolve signals for a polymer molecule existing in two different physical states depends on the rate of exchange of segments between these states,  $1/t_{exc}$ . In order to resolve these two signals  $t_{exc}$  must be greater than  $\tau_{tr}$ .

In most polymeric systems, the dominant relaxation mechanism for both  $T_1$  and  $T_2$  is the dipolar interaction between neighboring spins, modulated by molecular motion.

The form of the Hamiltonian for this interaction is

$$\mathcal{H}_{DD} = \frac{A}{r_{ij}^3} (1 - 3 \cos^2 \theta_{ij}) (\mathbf{I}_i \cdot \mathbf{I}_j - 3 I_{iz} I_{jz}) \quad (1)$$

For segments undergoing isotropic motion with short correlation times  $\theta_{ij}$ , the angle between an internuclear vector and the static magnetic field, is averaged over all possible values so that  $\langle (1 - 3 \cos^2 \theta_{ij}) \rangle$  tends to zero. Hence  $\mathcal{H}_{DD}$  is small for segments of high mobility in loops and tails. The theoretical limit for the spin–spin relaxation time, however, is not observed because polymer segments cannot reorientate isotropically in space. This leads to solution values of  $T_2$  in the range 10–500 ms.

However, for segments in trains the dipolar Hamiltonian is large, and this leads to very efficient relaxation and  $T_2$  values in the range 10–100  $\mu$ s are expected. Hence for an adsorbed polymer a superposition of two signals with widely differing time constants and intensities might be expected. In practice it is difficult to achieve a resolution in the line width parameter  $T_2$  of greater than 30 ms in these systems by a simple one-pulse sequence because of heterogeneous interactions. Fortunately, it is possible to separate the two contributions to the signal by a suitable combination of radio-frequency pulses.

In the pulsed NMR experiment variable-length pulses are used to change the orientation of the nuclear moments with respect to the static field. These pulses are thus acting on the spin vectors  $\mathbf{I}_i$  and  $\mathbf{I}_j$  of eq 1. A  $180^\circ$  pulse inverts any spin vector component (e.g.,  $I_x \rightarrow -I_x$ ); however, this produces no net effect on  $\mathcal{H}_{DD}$  as the pulse does not mix the orthogonal components. This means that for segments with long correlation times a  $180^\circ$  pulse has no net effect on  $T_2$  relaxation. However, a  $90^\circ$  pulse mixes the spin components (e.g.,  $I_x \rightarrow I_y$ ) and under certain circumstances the  $90^\circ_x - \tau - 90^\circ_y$  pulse pair can remove the first-order dipolar coupling, provided  $\tau \ll T_2$ . Hence the effect of the sequence is to increase the apparent  $T_2$ . For the detection of solid signals the  $90^\circ_x - \tau - 90^\circ_y$  technique has several advantages, including reducing the effect of the receiver recovery time. Provided there is a reasonable magnetic field homogeneity, both the  $90^\circ_x - \tau - 90^\circ_y$  and the

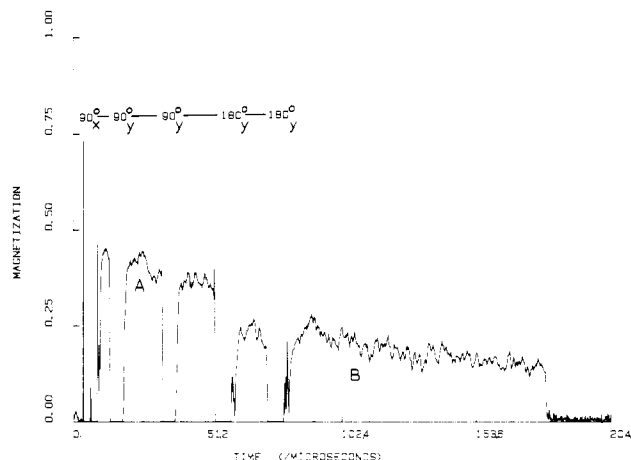


**Figure 1.**  $90^\circ_x - \tau - 90^\circ_y - 2\tau - 90^\circ_y - 2\tau - 180^\circ_y - 2\tau - 180^\circ_y$  sequence: PVP adsorbed on Aerosil dispersed in  $D_2O$  at 0.3 of a monolayer.  $\tau = 10 \mu$ s.

$90^\circ_x - \tau - 180^\circ_y$  sequences refocus the transverse spin components for loops and tails. In the present experiments both these sequences have been combined into a single pulse train:  $90^\circ_x - \tau - 90^\circ_y - 2\tau - 90^\circ_y - 2\tau - 180^\circ_y - 2\tau - 180^\circ_y$ ; this sequence is discussed in detail elsewhere.<sup>6</sup> The overwhelming advantage of this method of analysis, where the train segments are strongly adsorbed, is that there is no need to use curve-fitting methods which are necessary for deconvoluting single-pulse experiments and in other techniques such as ESR. The bound fraction,  $\langle p \rangle$ , is calculated from the first echo height (A) and the last echo height (B):

$$\langle p \rangle = 1 - B/A \quad (2)$$

### Experimental Section

A 60-MHz computer-controlled<sup>7</sup> pulsed NMR spectrometer was used in these experiments and spectra were signal averaged on a PDP11 minicomputer.

The nonaqueous dispersion consisted of graphitized Philblack "O" (specific surface area  $80 \text{ m}^2 \text{ g}^{-1}$ ) in carbon tetrachloride (redistilled Analar Grade) with adsorbed polystyrene (PS) (molecular weight 51 000;  $M_w/M_n \sim 1.1$ ). Adsorption equilibrium occurred after 24 h. The samples were slowly centrifuged and the supernatant was replaced by pure solvent. In this way all residual polymer was removed from solution: the spectra were then obtained immediately. The adsorbed amount corresponding to monolayer coverage was  $0.4 \text{ mg m}^{-2}$ . A sample of polystyrene (molecular weight  $\sim 10$  000) terminally anchored on Philblack "O"<sup>8</sup> dispersed in carbon tetrachloride was also prepared. All the segments in this system can be considered to be in tails.

The aqueous dispersions consisted of deuterio-hydroxylated silica ("Aerosil", surface area  $130 \pm 25 \text{ m}^2 \text{ g}^{-1}$ ) in  $D_2O$  with adsorbed poly(vinylpyrrolidone) (PVP) (molecular weight 44 000).

Adsorption equilibrium occurred after 12 h. In this system  $^1\text{H}$  impurities in both the silica and  $D_2O$  can contribute significantly to the signal. The residual solvent protons can be removed by taking advantage of their very long spin–lattice relaxation times ( $\sim 9$  s); this is achieved by a modification of the pulse sequence.<sup>6</sup> The contribution from surface OH groups is removed by digital subtraction of the signal from a standard silica dispersion with no added polymer.

### Results and Discussion

Figure 1 shows the spectrum obtained from PVP adsorbed on silica at a coverage of 0.3 of a monolayer ( $\theta_m$ ). The solid echo formed after the first  $90^\circ_y$  pulse contains signals from both the mobile and immobile populations. After the  $180^\circ_y$  pulse there is a substantial drop in signal intensity, showing the insensitivity of the immobile population to the preceding pulse. On this sweep time scale (204.8  $\mu$ s) there is no apparent decay of the liquid echo as

Table I

polymer	$\bar{M}_w$	substrate	solvent	$\theta_m$ coverage <sup>a</sup>	$\langle p \rangle$
PVP	44 000	silica	D <sub>2</sub> O	1.0	0.45 ± 0.15
PVP	44 000	silica	D <sub>2</sub> O	0.7	0.53 ± 0.1
PVP	44 000	silica	D <sub>2</sub> O	0.6	0.70 ± 0.1
PVP	44 000	silica	D <sub>2</sub> O	0.3	0.90 ± 0.18
PS	51 000	Philblack "O" <sup>c</sup>	CCl <sub>4</sub>	1.0	0.30 ± 0.05
PS <sup>b</sup>	10 000	Philblack "O"	CCl <sub>4</sub>	-	0.00

<sup>a</sup> I.e., fraction of a monolayer. <sup>b</sup> Terminally grafted.  
<sup>c</sup> Graphitized.

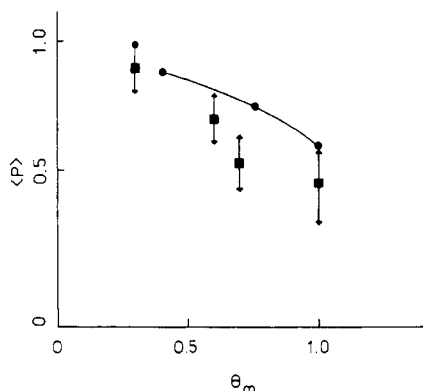


Figure 2. Variation of  $\langle p \rangle$  for PVP adsorbed on silica in D<sub>2</sub>O as a function of coverage (■). ESR results of Robb et al.<sup>3</sup> (●).

would be expected. The base line at the extreme right of the spectrum is obtained by changing to a very long sweep width. To reduce coherent noise and pulse breakthrough subsequent scans are phase alternated and this particular spectrum represents 1000 accumulations.  $\langle p \rangle$  estimates were obtained for several different samples on the adsorption isotherm, and the results are summarized in Table I and plotted in Figure 2. Also shown in the figure are ESR results<sup>3</sup> obtained for the same system. Qualitatively both techniques show the same overall trend of an increasing  $\langle p \rangle$  with reduced coverage. It would appear that the NMR values are systematically smaller than those obtained by ESR. Several factors may account for this, including some uncertainty in the amount of polymer adsorbed and the influence of the spin label on the adsorbed chain configuration.

At low coverages, both techniques show that over 90% of the segments of the adsorbed polymer are immobile. This value is considerably more than that obtained by infrared<sup>9</sup> but may be explained in terms of the mobility of segments close to, but not in, the surface. These segments will contribute to the train population in both NMR<sup>4</sup> and ESR measurements, suggesting a flat immobile layer at low coverages. At high coverages a distinct mobile population appears, due to the formation of extended loops and/or tails.

The second system chosen for study was a nonaqueous dispersion. Below monolayer coverage, polymer-stabilized dispersions of this type are unstable because of bridging flocculation and hence the only result presented here corresponds to a solution concentration just sufficient to give monolayer coverage (0.4 mg m<sup>-2</sup>). Above this polymer concentration the excess free polymer molecules in solution contribute to the spectrum, making accurate results dif-

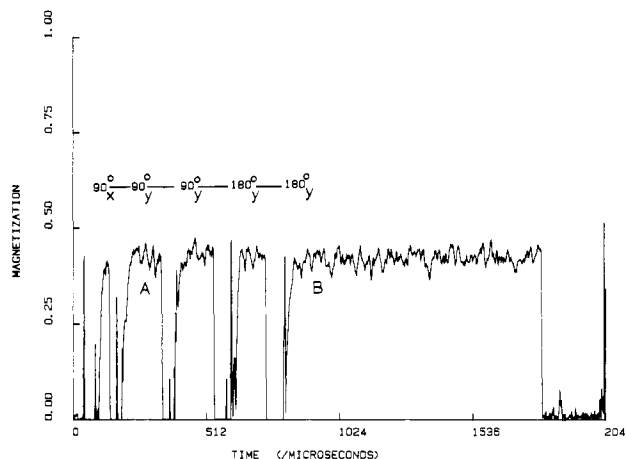


Figure 3. 90°<sub>x</sub>-τ-90°<sub>y</sub>-2τ-90°<sub>y</sub>-2τ-180°<sub>y</sub>-2τ-180°<sub>y</sub> sequence: polystyrene terminally anchored on Philblack "O".

ficult to obtain. The  $\langle p \rangle$  value for this dispersion (Table I) is 0.3 ± 0.05, which is somewhat less than the corresponding PVP/silica value (~0.8 mg m<sup>-2</sup>),<sup>10</sup> considering the differences in adsorbed amount. A smaller  $\langle p \rangle$  value may be attributed to the mechanism of the adsorption: on silica, PVP is adsorbed by hydrogen bonding between pyrrolidone groups and surface silanols, whereas in the nonaqueous system there is a weaker interaction, probably that between the phenyl groups of the polystyrene and the carbon surface.

Figure 3 shows the NMR spectrum obtained from the chemisorbed sample. In this case the observed  $\langle p \rangle$  value is zero, within experimental error, as would be expected from a sample made up entirely of tails, with no appreciable contribution from segments close to the surface layer.

The addition of a nonsolvent (deuterated methanol) to this dispersion causes an immediate flocculation. This is accompanied by a large reduction in the mobile component and a substantial increase in  $\langle p \rangle$ . However, because of heterogeneous broadening, an accurate  $\langle p \rangle$  value was impossible to obtain.

## Conclusion

NMR techniques have been used to measure  $\langle p \rangle$ , the bound polymer fraction, for both aqueous and nonaqueous dispersions. The measured values are consistent with the strength of the polymer surface interaction, and, in particular, the aqueous system gives values in qualitative agreement with published ESR values.

**Acknowledgment.** The Science Research Council is acknowledged for a grant toward building the NMR equipment and two CASE studentships with I.C.I. Corporate Laboratory.

## References and Notes

- Van der Linden, C.; Van Leemput, R. *J. Colloid Interface Sci.* **1978**, *67*, 48.
- Killmann, E.; Eisenlauer, J.; Korn, M. *J. Polym. Sci., Part C* **1977**, *61*, 413.
- Robb, I. D.; Smith, R. *Eur. Polym. J.* **1974**, *10*, 1005.
- Douglas, D. C.; McBrierty, V. J. *Polym. Eng. Sci.* **1979**, *19*, 1054.
- Kaufman, S.; Slichter, W. P.; Davis, D. D. *J. Polym. Sci., Part A-2* **1971**, *9*, 829.
- Cosgrove, T.; Barnett, K. G. *J. Magn. Reson.* **1981**, *43*, 15.
- Cosgrove, T.; Littler, J. S.; Stewart, K. *J. Magn. Reson.* **1980**, *38*, 207.
- Bridger, K. Ph.D. Thesis, University of Bristol, 1979.
- Day, J. C.; Robb, I. D. *Polymer* **1980**, *21*, 408.
- Cohen-Stuart, M. C. Ph.D. Thesis, Wageningen, 1980.